Digital Twins to Increase Mobility in Rural South Carolina

Final Report

Prepared by:

Dr. Paul Ziehl

Professor, Departments of Mechanical, Civil, and Environmental Engineering

University of South Carolina

301 Main Street, Ste. 3A41

Columbia, SC 29208

Office: (803) 467 4030

Email: ziehl@cec.sc.edu

Dr. Gurcan Comert

Associate Professor, Department of Physics and Engineering

Benedict College

Dr. Mahmoud Bayat

Research Associate Professor, Department of Civil and Environmental Engineering

University of South Carolina

May 2022

Center for Connected Multimodal Mobility (C²M²)

200 Lowry Hall, Clemson University Clemson, SC 29634

DISCLAIMER

The contents of this report reflect the views of the authors, who are responsible for the facts and the accuracy of the information presented herein. This document is disseminated in the interest of information exchange. The report is partially or entirely funded by the Center for Connected Multimodal Mobility (C^2M^2) (Tier 1 University Transportation Center) Grant, which is headquartered at Clemson University, Clemson, South Carolina, USA, from the U.S. Department of Transportation's University Transportation Centers Program. However, the U.S. Government assumes no liability for the contents or use thereof.

Non-exclusive rights are retained by the U.S. DOT.

ACKNOWLEDGMENT

Technical Report Documentation Page

1. Report No.	2. Government Accession No.	3. Recipient's Catalog No.
4. Title and Subtitle Digital Twins to Increase Mobility in Rural South Carolina		**5. Report Date**
		6. Performing Organization Code
7. Author(s) Paul Ziehl, Ph.D. ORCID: https://orcid.org/0000-0002-4783-9255 Gurcan Comert, Ph.D. ORCID:https://orcid.org/0000-0002-2373-5013 Mahmoud Bayat, Ph.D. ORCID: https://orcid.org/0000-0002-0990-7077		**8. Performing Organization Report No.**
9. Performing Organization Name and Address University of South Carolina, 300 Main St, Columbia, SC 29208		**10. Work Unit No.**
		11. Contract or Grant No. 69A3551747117
12. Sponsoring Agency Name and Address Center for Connected Multimodal Mobility (C2M2) Clemson University 200 Lowry Hall, Clemson, SC 29634		**13. Type of Report and Period Covered** Final Report (October 2020-June 2022)
		14. Sponsoring Agency Code
15. Supplementary Notes		

16. Abstract

A Digital Twin (DT) approach is proposed as one potential step to the development of an autonomous (or semi-autonomous, referred to as 'autonomous' henceforth) load rating procedure for precast reinforced flat slab concrete bridges. The load rating is an approach to address the load-carrying capacity of in-service bridges. Full-scale laboratory testing was conducted on a bridge slab that was extracted from a de-commissioned bridge. The ultimate moment capacity of the slabs was assessed through the implementation of a bending test. The slabs were instrumented with strain and acoustic emission sensors to capture crack propagation and strain under a stepped loading procedure. Finite element modeling and the model calibrated in the experimental study under different loading conditions were conducted. A digital twin of a single slab of a precast flat slab bridge near Abbeville, SC, was developed. Different scenarios were examined to obtain an enhanced understanding of the behavior of one precast reinforced flat slab span. Field investigations were conducted, and the response of the bridge under daily traffic loading was utilized for calibration of the digital twin. The approach does not need any road closure and is cost-effective.

17. Keywords Digital Twin, Load rating, Flat slab bridges		**18. Distribution Statement**	
19. Security Classif. (of this report) Unclassified	**20. Security Classif. (of this page)** Unclassified	**21. No. of Pages**	**22. Price** NA

Table of Contents

Center for Connected Multimodal Mobility (C²M²)
Clemson University, Benedict College, The Citadel, South Carolina State University, University of South Carolina

iv

LIST OF TABLES

LIST OF FIGURES

EXECUTIVE SUMMARY

The South Carolina Department of Transportation (SCDOT), along with all state DOTs and those who utilize the transportation infrastructure, are living in interesting times. Rapid technological advances are taking place in private mobility sectors, including automotive and flight, spurred on by substantial investments in Defense by the United States and near peer adversaries from many decades ago. Advances include 'autonomy and electrification of everything' with numerous examples in vehicle-to-vehicle and vehicle-to-infrastructure communications. Additionally, the most substantial investments in transportation infrastructure were made in the 1950s when traffic was far lighter, and truck weights were approximately one-half of those today. As vehicles become electrified, the weight of the batteries needed to propel them will only add to issues of overloading. A significant reduction in funding for infrastructure assessment and maintenance compounds these issues. It is safe to say that roads and bridges in general, particularly bridges in rural areas, have not benefited from the next technological revolution. In fact, the situation is very much the opposite.

The SCDOT is in the process of load rating all bridges in its substantial inventory. The load rating is a federally mandated process to calculate bridge capacity. Approximately one-third of South Carolina's bridges were designed for much lower loads, H-10 (20,000 lb. vehicles) and H-20 (40,000 lb. vehicle), than they experience. For this reason, many bridges will not rate satisfactorily and will therefore be load restricted, requiring truck traffic, emergency vehicles, and school buses to be rerouted. The typical resolution is strengthening or replacement, both at a substantial cost. In this project, a Digital Twin (DT) approach is proposed to define the load-carrying capacity of an as-built bridge plan, which includes the development of an autonomous (or semi-autonomous, referred to as 'autonomous' henceforth) load rating procedure for precast reinforced flat slab concrete bridges. Full-scale laboratory testing was conducted on a bridge slab that was extracted from a demolished bridge. The ultimate moment capacity of each slab was assessed through the implementation of a four-point bending test. The slabs were instrumented with a series of strain gauges and acoustic emission sensors to capture crack propagation and the existing strain of the slabs under the loading procedure. 3D-finite element modeling was also generated and calibrated with the experimental study under different loading conditions. A digital twin of the flat slabs was developed through calibrated laboratory testing and numerical modeling. Abbeville Bridge in South Carolina was also instrumented and tested under daily traffic loading conditions, and the results are presented. Different scenarios are examined to provide an enhanced understanding of one load rating approach for precast reinforced flat slabs. The load rating factor is presented based on the SCDOT bridge evaluation guidance. One of the great advantages approach is that it does not require a road closure.

CHAPTER 1:
Introduction

One of the common approaches to evaluate bridges is by using simplified models that represent the structural dimensions and properties obtained from the original design plan during the on-site inspection. Since most of the bridges in the United States were built years ago, it is common to have bridges with no structural plans (ASCE, 2013) or structural plans that may vary from as-built conditions. The performance of any bridge decreases during its service life due to varied reasons, such as corrosion in reinforcement, cracks in concrete, and concrete strength reduction (Islam et al., 2015). Load rating seeks to express the load carrying capacity of a bridge through a rating factor (R.F.). Where plans are adequate or helpful, alternative means must be utilized. Two such methods described by the American Association of State Highway and Transportation Officials (AASHTO) Manual for Bridge Evaluation are engineering judgment and proof testing (AASHTO, 2019). However, engineering judgment creates a degree of risk both on the side of unconservative and conservative estimations. Proof testing may lead to damage and is often costly (Alampalli et al., 2021). The time required for the on-site inspection and load rating typically ranges between one to four days, which generally involves the closure of lanes and leads to traffic congestion. These lane closures are required for both the safety of the inspectors and due to the size of the equipment used to identify and classify deficient portions of the bridge. The finding of deficiencies leads to an increased frequency of inspections and thereby increases costs (Zulifqar et al., 2014).

The effectiveness of bridge inspections should increase by making the bridge inspection ratings more objective and accurate. The total inspection cost should be minimized by eliminating traffic control costs and reducing labor and equipment costs. Moreover, there is a need to remove the safety risk of personnel in bridge inspections. The prominent objective is to reduce the cost and time of inspections while maintaining and/or increasing inspection quality by making it objective and safe for users (ARTBA, 2020). The AASHTO (2019) states that "Many older reinforced concrete and prestressed concrete beam and slab bridges whose construction plans, design plans, or both are not available, need proof testing to determine a realistic live load capacity." Current load rating approaches are described in Lantsoght et al., 2017.

The proposed approach (Digital Twin) is relatively new for bridge assessment and can significantly reduce time and resources in extensive instrumentation, specialized loading, and traffic control are not required. The approach has become feasible due to advances in data-driven assessment techniques (artificial intelligence) combined with advances in connectivity. The benefits will include tremendous cost savings to the SCDOT realized through a reduced number of bridge replacements or strengthening, combined with increased mobility of freight (trucks) and other vehicles such as fire trucks, ambulances, and school buses. Rural communities will be the greatest beneficiaries, as the majority of load-restricted bridges serve these communities.

The impacts will be realized over the longer term as new approaches to transportation infrastructure assessment are realized through vehicle-to-infrastructure communications and bridge assessment. This will lead to fruitful datasets in terms of infrastructure response to well-

Center for Connected Multimodal Mobility (C²M²)
Clemson University, Benedict College, The Citadel, South Carolina State University, University of South Carolina

1

understood vehicular loading, with only minimal instrumentation of the transportation infrastructure itself.

CHAPTER 2:
Literature review

2.1 Digital Twins

This section summarizes current practices related to digital twin technology, specifically related to bridge modeling. Liu et al. (2020) discussed safety evaluations with data from digital twins for prestressed steel structures. A digital twin is a mirror of the structure in digital space and can provide information on the structure's behavior, such as strength in real-time. This is first done by loading the structure with sensors. These sensors collect data so a virtual 3D model of the structure can be made. The authors discussed the use of Support Vector Machines (SVM). This SVM and digital twin collectively lead to a safety risk assessment model. The case study discussed in this paper was a wheel-spoke cable truss. This is a prestressed steel structure that resembles the shape of a bicycle wheel. The main components that will affect this structure during its service life are loading, temperature effects, and corrosion.

This demonstrates the importance of assessing the safety which can be done efficiently by digital twin modeling. In their study, an experimental model was built to be instrumented. This model had a ratio of 1:10 compared to the actual truss, and the cables cross-sectional area had a ratio of 1:100. The model structure had a span of 19.6 ft (6 mt) and included ten radial cables. All materials used were that of the actual physical truss, and a virtual model was created as well. After the construction of the model, it was instrumented with sensors to collect data. This data was reflected in the virtual model creating synchronization between the virtual and physical models. The data that was collected from this smaller model was input into the system to train a Support Vector Machine (SVM) model and allow risk prediction of the actual physical structure. The purpose of the study was to investigate the use of digital twins to establish the safety level of prestressed steel structures. The SVM algorithm was used to predict structural safety level, which was then used to build an evaluation system. Digital twins can make the structure safer while it is still in use by collecting data in real-time to make the structural assessment and evaluate the risks. This in turn improves the efficacy/efficiency of the evaluation process.

Ye et al. (2019) focused on the importance of bridges. For these bridges to do their job, they need to be maintained and able to adapt to changing conditions. The problem they faced was processing and evaluating the mass data collected, which can be timely and costly. The objective of digital twins is to combat this issue directly. The digital twin can be constantly updated and provide feedback using predictions that can be deduced about the behavior of the actual/physical structure with changing conditions. The paper discussed a two-year study involving two bridges. The purpose of the study was to assess different approaches to the problem. The framework for creating the digital twin for bridges was proposed. A Bridge Information Model (BIM) can be used to find issues within the data and visualize the stress-strain distribution.
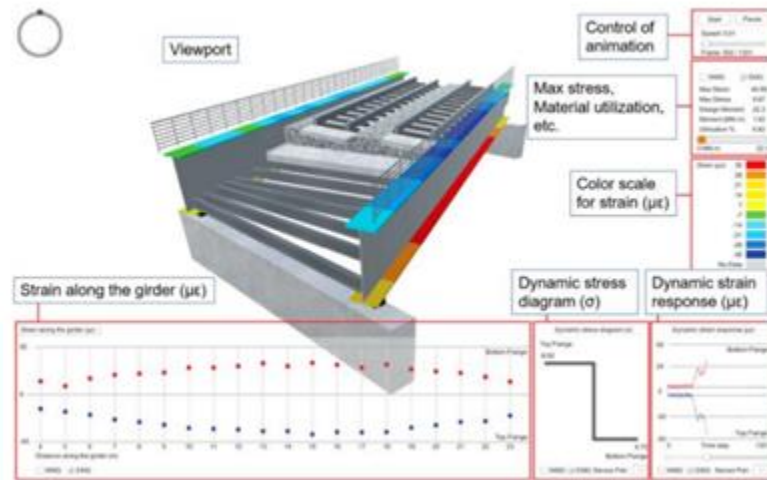
Center for Connected Multimodal Mobility (C²M²)
Clemson University, Benedict College, The Citadel, South Carolina State University, University of South Carolina

3

Figure 2.1 BIM model (Ye et al., 2019)

A challenge with beginning a digital twin is sifting through the large datasets and finding valuable information that can be used for decisions on safety assessment.

A BIM model was developed showing strain and stress along the girders in the bridge when a train passes over. Data collected from sensors instrumented on the bridge was used to build a finite model. This led to the creation of a 3D FE model. The FE model was verified by the strain measurements that were collected in the BIM. Data-driven approach scrambles the sensor data collected during train passage events, and with the use of statistical modeling, errors, and patterns were found. The Data-Centric Engineering (DCE) approach is introduced in the article. This approach can minimize systematic errors and combine many different datasets to produce a digital twin to find the structural health assessment of the bridge. The paper emphasized that integrating multiple data simulation models (BIM, FE, and statistical) is crucial to have more confident predictions.

Digital twins to improve and prevent maintenance within the bridge industry were discussed by Shim et al. (2019 a, b). The authors proposed image processing for inspection and a 3D information model for the future of the bridge maintenance process for prestressed concrete bridges. It is preferred to have 3D models for each stage of the bridge, design, construction, operation, and maintenance. The paper pointed out that short-span bridges do not have regular maintenance, making them more expensive to operate.

In 2017, the U.S. Infrastructure Report Card announced that 9.1% of bridges were structurally deficient (ASCE infrastructure report card (2017)). Along with this, many bridges are beginning to reach their design life, and we can expect deterioration if the maintenance process is not improved. The lifetime reliability index is what we want to find here because it covers the load-rating factor and models of deterioration. With the creation of lifetime functions, predictions can eventually be made about the structure. Computing a time-dependent performance indicator also assists the prediction model, which covers vulnerabilities of the structure due to many factors. Many deterioration models have already been created based on data from bridges currently

Center for Connected Multimodal Mobility (C²M²)
Clemson University, Benedict College, The Citadel, South Carolina State University, University of South Carolina

4

deteriorating, however, this is not the case for lesser spans (ASCE infrastructure report card (2017)).

Shim et al. (2019 a, b) recommended a BIM model in combination with a surface model that is scanned. All historical data on the bridge, including past inspections and damages, should also be uploaded into the system to aid in the maintenance process for the entire lifecycle of the bridge. An analysis model can be made from the data of the bridge's deterioration history. First, a 3D geometric model needs to be created. A surface model can then be created with the use of UAV scanning. Data will be received to create an analysis model to allow predictions. The goal of the DTM is the long-term management and operation of the bridge. Inspections can be made from the automated data capturing system leading to a safer structure because more frequent inspections can be made. Maintenance work includes inspecting, monitoring, and repairing. For this purpose, many cable-supported bridges already have sensors to monitor damage, but the repairs are not managed effectively. Some of the major concerns for cable-supported bridges are fatigue, corrosion, and connection failure. This study introduced using digital twins to make this process more effective. The digital model collects data and creates a more organized history of damage and repairs. This will lead to cost savings because it can enhance the design. An interface system is to be developed that can go through all the data received from the structure during design, construction, service life, and maintenance and find the patterns through mathematical and empirical models to make predictions for future behavior. It is crucial that the digital twin is updated in real-time.

Figure 2.2 Digital twin models (Shim et al.,2019b)
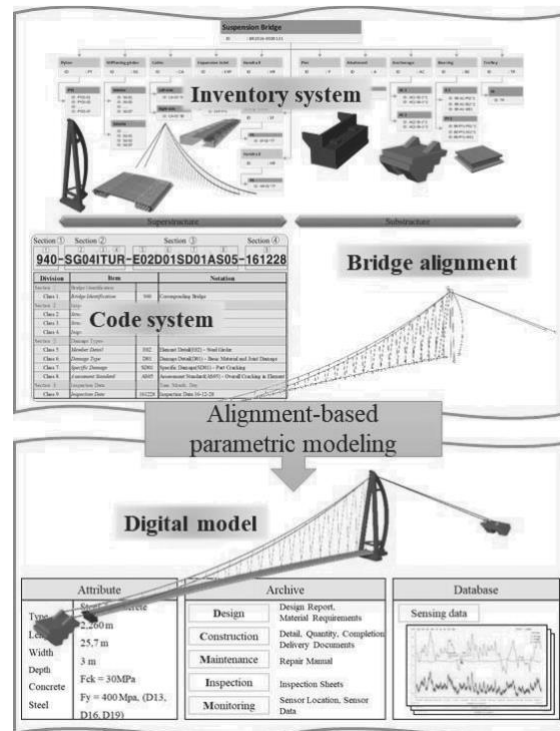
(Figure courtesy of the Institute of Civil Engineers)

Center for Connected Multimodal Mobility (C²M²)
Clemson University, Benedict College, The Citadel, South Carolina State University, University of South Carolina

5

Until now, sensors have not been used to update the BIM maintenance system in real-time, as the data has been historically based. Disadvantages, as a result, include challenges for analysis of the data and local damages not being well established. An important aspect of DTM is that it can hold data for the entire life cycle of a bridge. With the model reflecting real-time responses, the future performance of the structure can be predicted, and the maintenance processes can be improved.

Lu et al. (2020) included a detailed case study using the West Cambridge Campus to demonstrate the use of digital twins on the city level. A city-level digital twin would include several sub-digital twins that would represent the buildings within the cities. Benefits of bringing DTs to the city level include optimization of maintenance costs, determining energy demand, connecting society to the structural health of the infrastructure, and bringing attention to the operation and maintenance of the infrastructure of the city. This case study used many different data collection systems and transferring technologies for the various sub-DTs, which then created the challenge of integrating each of these to create the large city DT. The paper specified all the different data acquisition, analysis, transmission, and integration technologies that are used to create a successful DT that can be used to improve the operation and maintenance of cities, and therefore, service to society.

Lin et al. (2019) considered a case study done on a skewed half-through railway bridge that was instrumented with 108 fiber optic sensors during the time of construction and analyzed during the beginning months of service. Data on strain measurements during train passage events from the sensors for the main girders and crossbeams were compared and analyzed. A 3D-finite element model was created in support of these results. They found that it was acceptable to simplify the creation of this model by using concentrated loading when assessing structural behavior rather than distributed load distribution. When comparing the two behaviors of the bridge under each of the loading scenarios, they behaved very similarly. The FE model successfully predicted the load distribution within the girders and crossbeams and could confidently be used in the future to assess the fatigue of the structure. It was also discovered that there was great eccentricity within the bridge as the strain measurements within the girders showed a significant difference in load sharing. The load rating capacity was analyzed with the strain results, and it was concluded that the bridge was only using 37% of the structural capacity. This study also compared the strain effects within the two different connections, moment and pinned, at the end of the cross beams and found they were similar. The case study was successful in proving the great benefits of the instrumentation of bridges and the creation of finite element models to assist the structural assessment and design of bridges.

Butler et al. (2018), summarized the results from a case study done in the United Kingdom on a 26.8 m steel half-through railway bridge instrumented with fiber optic sensors (FOS). It is important to note this bridge was instrumented during construction (9 months), which decreases the unknown variables you are working with and provides an entire loading history for the future of the bridge structural health assessment. Fiber Bragg grating (FBG) sensors were placed on the bridge throughout the construction and provided data on the mechanical strain and temperature strain at various stages of construction.

The measurements taken from the sensors were compared to a finite element model created by the software system DIANA 10.1 (Butler et al. (2018)). The only loads calculated into the FE model were permanent loads, such as the self-weight of the bridge. The FE model was continuously updated throughout the construction process as parameters, permanent loads, and properties changed. The major factor influencing the strain of the curing period was a thermal strain. This strain followed a diurnal variation by decreasing during the night and increasing during the day, reaching its maximum strain. The mechanical strains followed this pattern as well at a lower level. Figure 2.3 illustrates strains during the curing process.
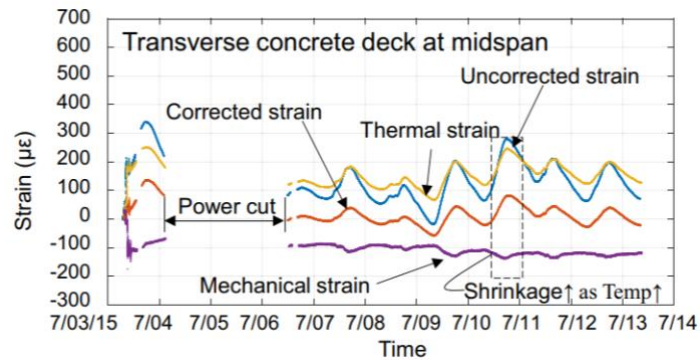

Figure 2.3 Strains during curing (Butler et al. (2018))

Top flange strains were underestimated, and bottom flange strains were overestimated (Figure 2.4). This is most likely due to the assumption that there were full moments at the connections. To assess the main girders and cross-beam, the results of flexural strain from both the FOS and FE models were integrated and an assumed value for flexural stiffness was used. Lateral-torsional buckling was accounted for during these calculations, and the results for the various FE models were compared to the sensors. The entire structure did not come close to the design capacity, which was to be expected since the study only considered dead permanent loads.

Center for Connected Multimodal Mobility (C²M²)
Clemson University, Benedict College, The Citadel, South Carolina State University, University of South Carolina
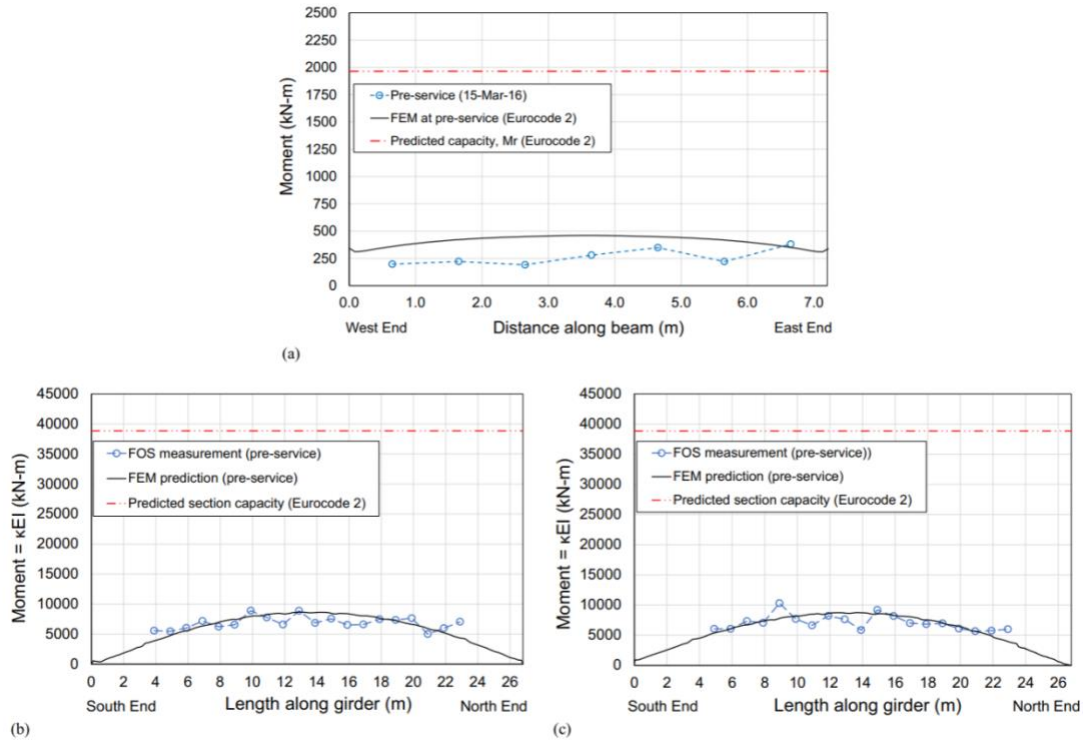
7

Figure 2.4 Moment distributions – measured and predicted: (a) beam (composite); (b) girder (west main); and (c) girder (east main) (Butler et al. (2018))

The paper (Butler et al. (2018)) pointed out the unreliability of thermal strains that were measured due to their variability based on night and day. Some parts of the structure also had larger thermal strain due to direct sunlight and could have lagged in measuring actual surface strain. Also, the transfer of thermal strain may not have been properly recorded. In reality, these thermal strains would have been non-uniform.

Based on measurements gathered from the sensors during the process of 10-day curing, it could be concluded that the nonuniform strains produced by the structure remained within the concrete deck. Overall, the FE model was close to the FOS measurements expected of the various nonuniform strains due to temperature gradients, thermal strain transfer, and concrete shrinkage. Din-Houn Lau et al. (2018) developed statistical tools and models that are needed to process large sets of strain data collected from the 134 fiber optic sensors. These sensors collected data at 250 Hz. The batch method was utilized to retrieve data collected when a train passed. This allows for the data to be reduced and ignores the strain data gathered from environmental effects such as temperature. The predicted statistical models are updated   Data that greatly deviated from the average could be labeled as anomalous.

Center for Connected Multimodal Mobility (C²M²)
Clemson University, Benedict College, The Citadel, South Carolina State University, University of South Carolina

8

2.2 Load Rating procedure

The load rating is currently approached through a combination of Diagnostic Load Testing and Proof Load Testing (Lantsoght et al., 2017).

2.2.1 Diagnostic Load Testing

In diagnostic load testing responses of key structural components to known test loads are measured. Typically, an analytical model is developed to enable comparisons (Fu et al., 1997; Hernandez et al., 2018; Kim et al., 2009). The proposed method (described later) does not require lane closures and provides continuous feedback of structural response.

2.2.2 Proof Load Testing

Proof load testing is a procedure developed to illustrate the ability of a bridge to carry applied loads (Aguilar et al., 2015; Anay et al., 2016; Casas et al., 2013; Lantsoght et al., 2017a,b). Proof testing (e.g., loading of the bridge with very heavy trucks) is costly, requires traffic control, and is challenging for prestressed structures. Automated evaluation methods, including structural monitoring, would hence be of great benefit to enhance mobility.

Center for Connected Multimodal Mobility (C²M²)
Clemson University, Benedict College, The Citadel, South Carolina State University, University of South Carolina

9

Chapter 3:
Methodology

In this section, a flexural test is described with acoustic emission data collected during the experiment. An ANN was developed to identify the load steps using the recorded acoustic emission data. A field investigation was conducted on a realistic bridge and its results were compared with the results of the experiment.

3.1 Laboratory testing

A four-point flexural test (ASTM, C1399) was set up and utilized in the laboratory. The experimental test setup of the original slab is presented in Figures 3.1 and 3.2. Figure 3.3. A special loading frame was used to test the specimens. The slab type is commonly used in rural South Carolina bridges. A rectangular seat was placed between the hydraulic jack and the steel plate to avoid uneven application of load. The specimens were loaded centrally up to the failure of the concrete in compression. A string potentiometer was used at the midspan of the slab to measure vertical displacement. The experimental test setup information can be found in Table 3.1.

Two LVDT sensors measured vertical and horizontal displacement. A 100-kip capacity load cell was used and located between the hydraulic ram and the spreader beam, as shown in Figure 3.3. Two loading scenarios were utilized for a slab in the test procedure. In scenario 1, three Bridge Diagnostics, Inc. (BDI) gauges were attached on the midspan of the slab top surface to obtain the strains. Four Acoustic Emission (AE) sensors were also installed to capture crack initiation. The load versus time curve is presented in Figure 3.4. In scenario 2, the same specimen was loaded to failure. The means of load application is shown in Figure 3.3.
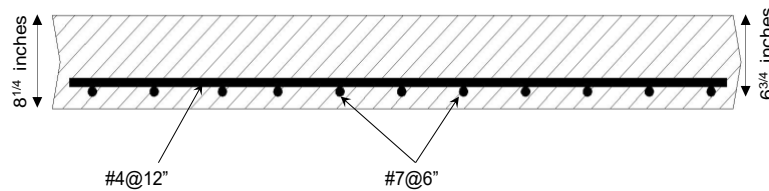

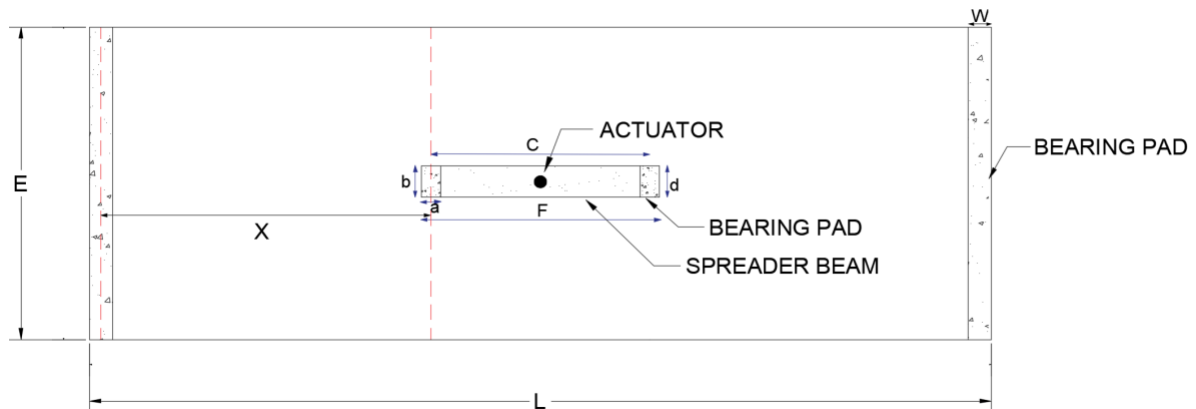**Figure 3.1 Dimensional information and reinforcing details**

Figure 3.2 Plan view of 15' slab test set up

Table 3.1 Experimental test set up information

L (ft)	E (ft)	D (in)	Support condition	W (in)	a (in)	b (in)	A (a*b) in²	c (in)	D (in)	F (in)	X (ft)
15	5.5	8.25	Bearing	9.5	8.5	8.5	72.3	40	8.5	51.7	5.43

Figure 3.3 Laboratory testing of precast reinforced flat slab

Figure 3.4 Load versus time curve

Center for Connected Multimodal Mobility (C²M²)
Clemson University, Benedict College, The Citadel, South Carolina State University, University of South Carolina
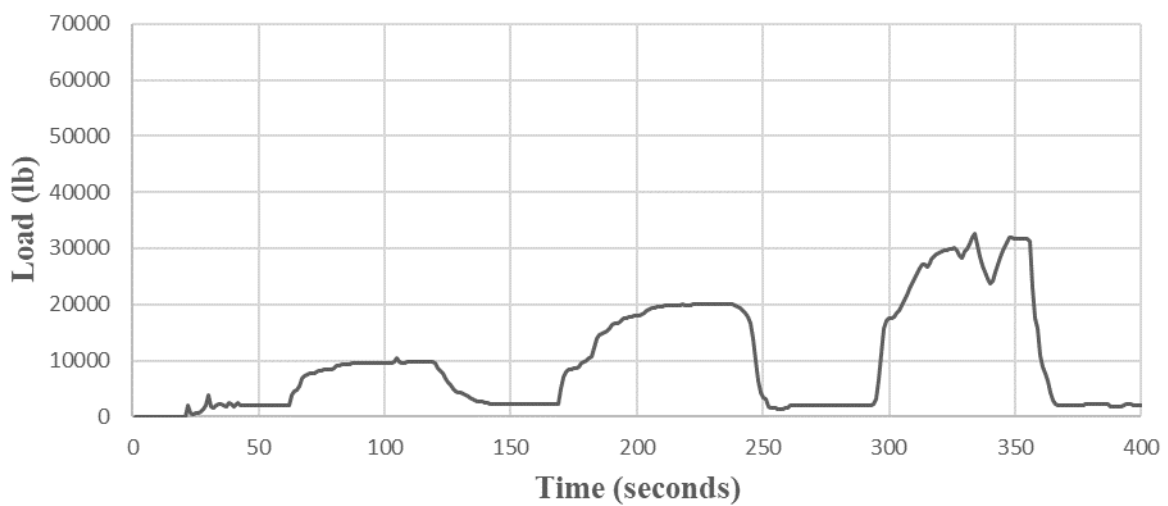
11

3.2 Numerical Investigation

A three-dimensional numerical model of the flat slab test was generated in ABAQUS. The geometry of the slabs and the bearing supports reflected the experiments. The slab was modeled with brick elements having eight nodes and reduced integration. Reinforcement was modeled with linear elements (B31). The typical mesh size of the concrete was 1" x 1" x 1". Details of the model are provided in Figure 3.5. The elastic modulus for the reinforcement was set as 29,000,000 psi, and the Young's modulus of concrete was assumed to be 3,605,000 psi.

The constitutive law of concrete employed in the model representing compressive and tensile damage is shown in Figure 3.6. Two loading scenarios were applied to the model. A simplified loading versus time curve was utilized (Figure 3.7) to reduce the computational complexity.
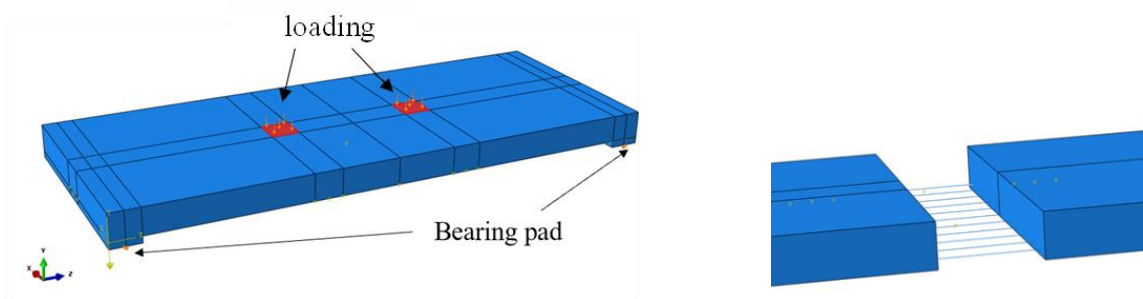

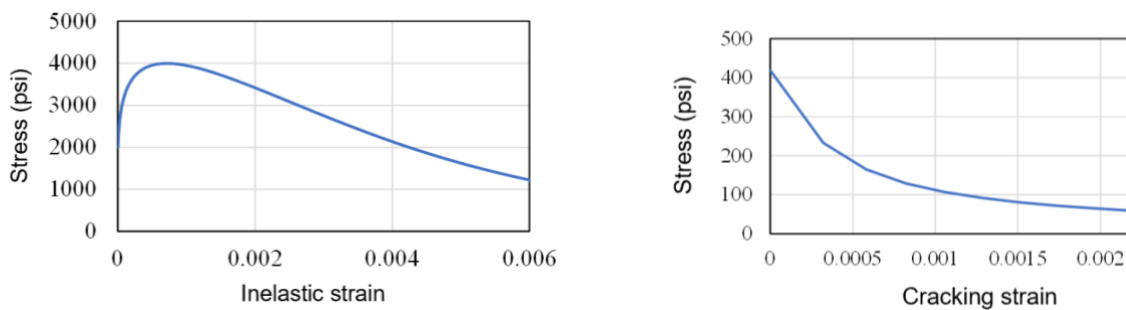**Figure 3.5 FE model and reinforcing details**

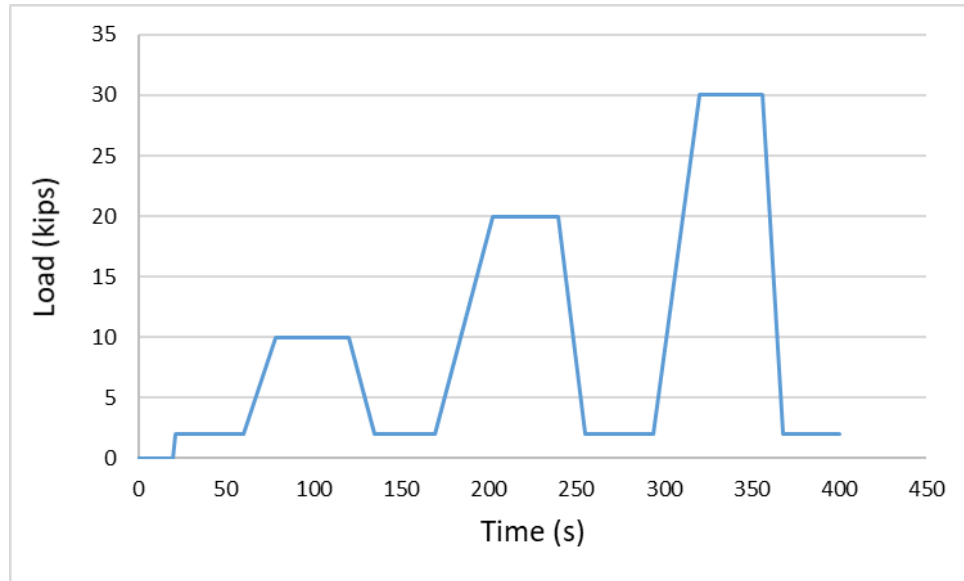**Figure 3.6 Constitutive law of concrete damage**

Figure 3.7 Idealized load vs. time curve

3.3 Experimental Results and FE Model Verification

Midspan strain and moment displacement curves were extracted with results presented in Figure 3.8. The red stripes on the concrete slab represent tensile cracks. The moment versus midspan displacement curve is shown in comparison to the experimental result. Reasonable alignment of the trends of the curves can be observed in the FE and experimental results in terms of strain (Figure 3.9) and mid-span moment (Figure 3.10). The yielding moment of the slab acquired by the FE model and the experiment are, respectively, 228 ft-kips and 211 ft-kips. The ultimate moment of the slab obtained by the FE model and the experiment is 247 ft-kips and 254 ft-kips.
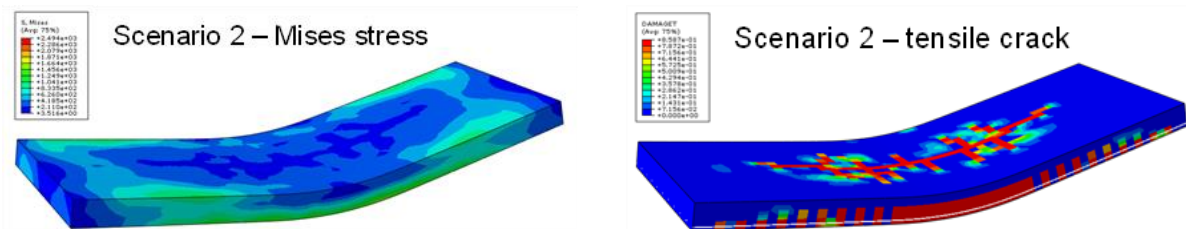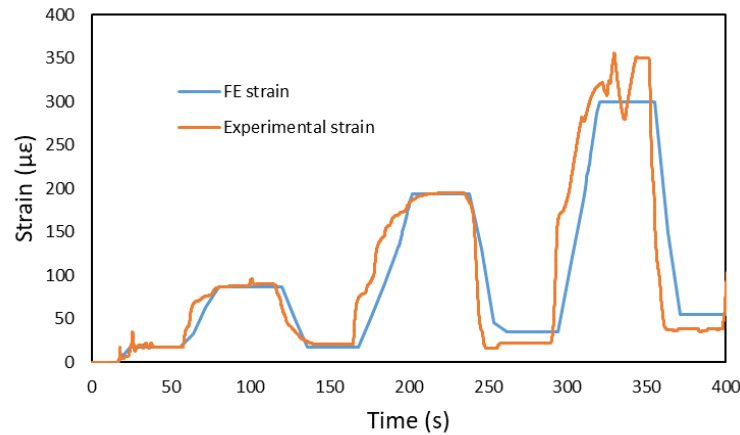

Figure 3.8 Modeling results

Center for Connected Multimodal Mobility (C²M²)
Clemson University, Benedict College, The Citadel, South Carolina State University, University of South Carolina

13

Figure 3.9 Comparison of FE model and experimental results: Strain versus time
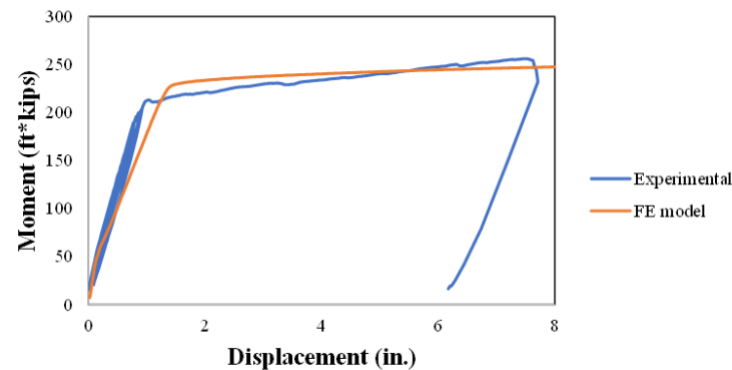

Figure 3.10 Comparison of FE model and experimental results: moment versus displacement

3.4 Acoustic Emission Data

Acoustic emission (AE) is a physical phenomenon that is essentially stress waves initiated by damage growth or similar sources. As micro- or macro-cracks occur within the structure, the AE sensors will respond to the associated stress wave, and this response is often referred to as a 'hit'. A typical captured waveform has many different attributes that allow researchers to categorize each hit. Acoustic emissions data were continuously collected during flexural testing. Broadband sensors were selected due to having a wide range of operating frequencies which can be helpful for waveform analysis. The sensors were placed at L/3 and W/3 locations, as shown in Figure 3.11.
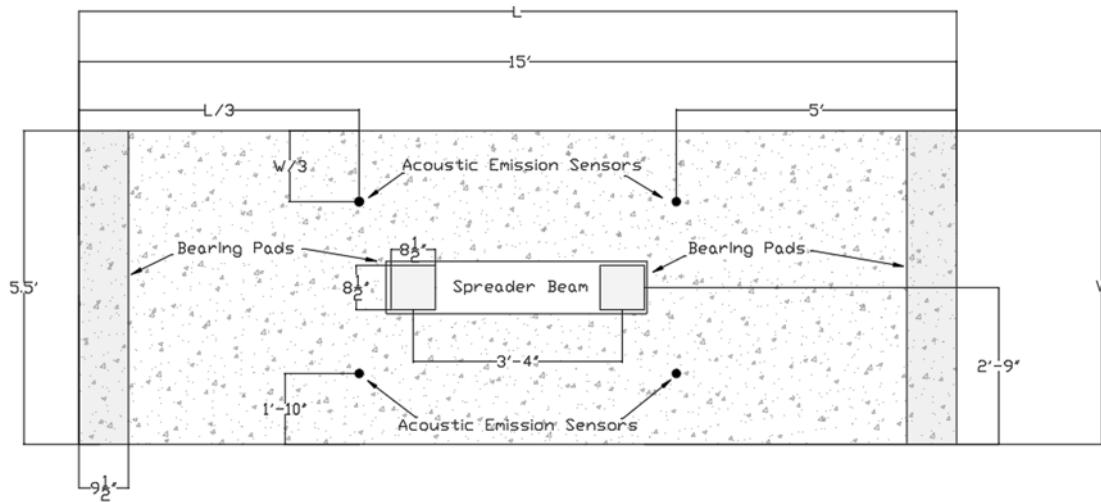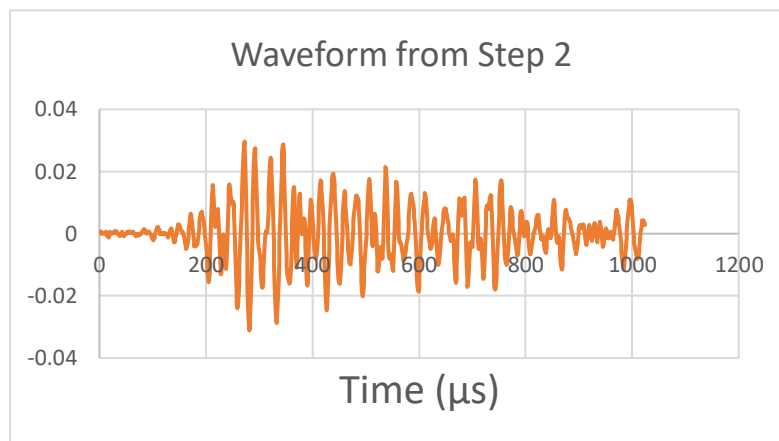
Figure 3.11 Test setup (plan view) showing AE sensor locations

Data was collected with a threshold of 50 decibels. The acquisition system collected over 23,000 waveforms from the test, and 13 different attributes (or features) were associated with each hit. The flexural test consisted of a stepped loading procedure. The slab was initially loaded to two kips, and then the load was increased to 10 kips (referred to as load step 1); unloaded to the baseline to two kips; loaded to 20 kips (referred to as load step 2); and then continued in this fashion to a maximum of 60 kips.

The analysis of the AE hits focused on determining differences between data collected during load step 2 (20 kips) and load step 3 (30 kips). Visual differences can be seen between a step 2 waveform and a step 3 waveform, as shown in the following figure.
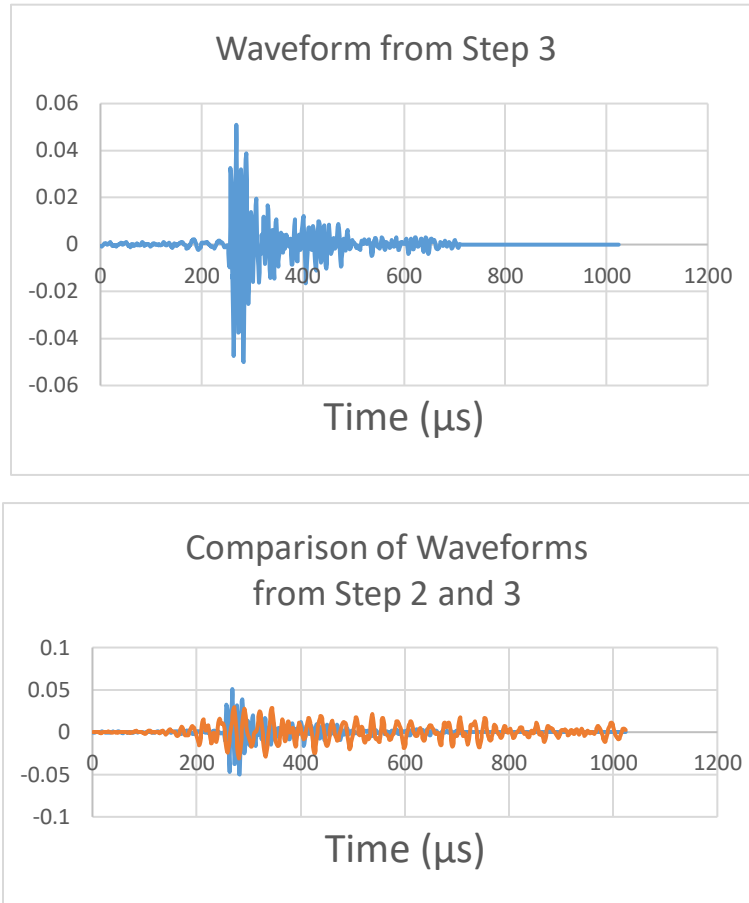

Center for Connected Multimodal Mobility (C²M²)
Clemson University, Benedict College, The Citadel, South Carolina State University, University of South Carolina

15

Figure 3.12 Wave forms from different load steps

The differences can also be compared using AE features such as amplitude, rise time, and many others. Definitions for AE features may be found in user's manuals that accompany the AE data acquisition system

Features such as amplitude, rise time, and energy were individually compared to determine if differences could be detected using only one or a few of these features. Various plots were created to visually represent the differences between the load steps.
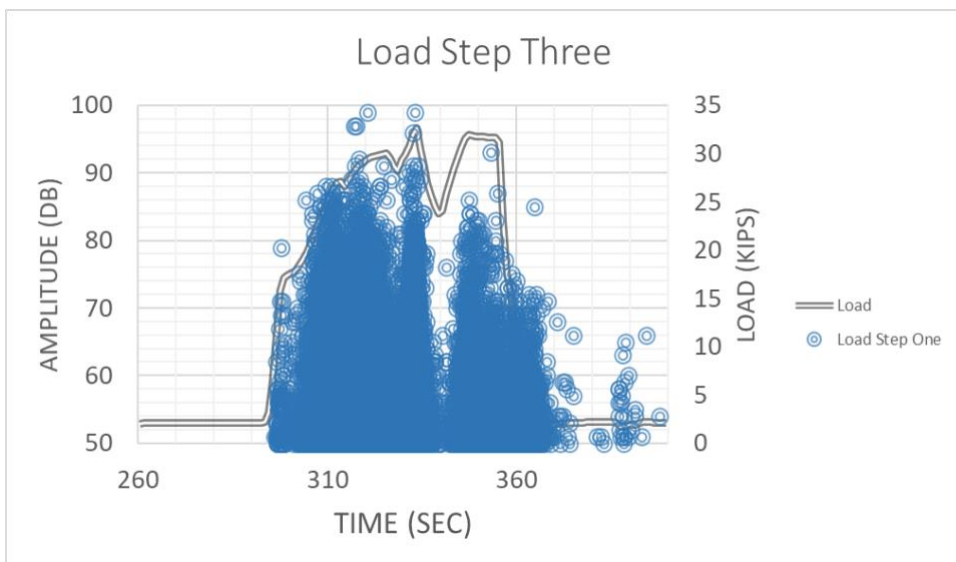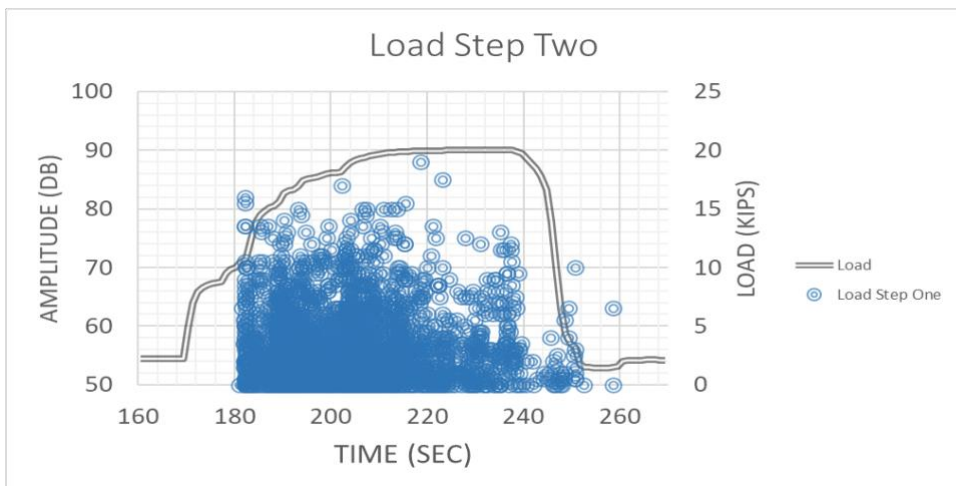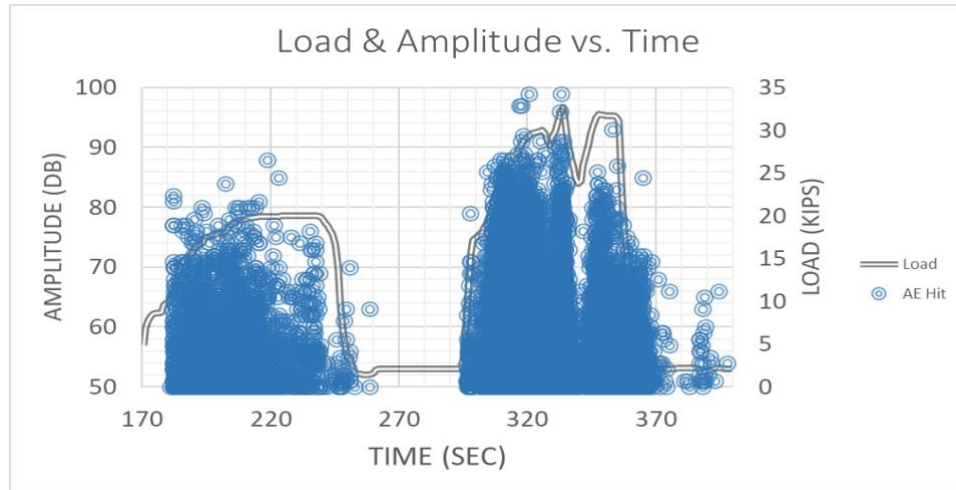
Load & Amplitude vs. Time

Load Step Two

Load Step Three

Center for Connected Multimodal Mobility (C²M²)
Clemson University, Benedict College, The Citadel, South Carolina State University, University of South Carolina

17

Figure 3.13 Load and amplitude vs. time for load steps 2 and 3 (top), load step 2 only (middle), and load step 3 only (bottom)

3.4.1 Artificial Neural Network (ANN) Implementation

While visual comparisons may be effective for determining general differences between load steps, it is not an efficient way of determining or classifying differences between waveforms. To address this, a neural network of the artificial type (ANN) was developed to classify waveforms based on all 13 features collected.

An ANN is inspired by biological neural networks, mimicking the way the human brain processes information. The idea is motivated by the desire for a program to solve natural or intelligent tasks using advancements in computing technology. An example of a 3-layer ANN is shown in the figure below. An ANN was used to predict the load steps on the slab. The AE signals (over 23,000 signals) collected during the experiment were utilized as the input if the ANN. The output of the ANN is the index of load steps (e.g., step 2 or step 3).
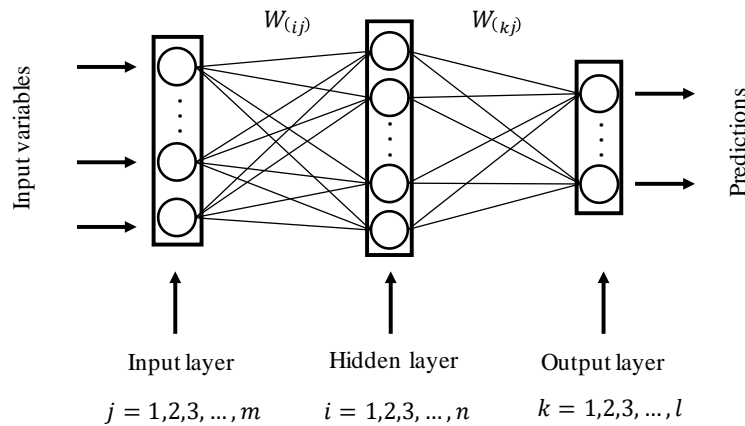

Figure 3.14 Example structure of a 3-layer artificial neural network

An imbalance issue occurred while training the neural network as the data points belonging to load step 3 outnumbered those belonging to load step 2 by almost 10:1. To address this, a code was created that randomly divided load step 3 data into ten groups. Ten different models were trained with load step 2 data and one-tenth of the load step 3 data. These models were then tested on a randomly selected group of data from load step two and load step three. The models then voted, and the majority rule determined the overall classification of the data point.

The performance of a neural network depends on its structure. The code was run 10 times with neurons ranging from 20 to 30 and an average accuracy was taken, resulting in an optimum number of 22 neurons. The same process was applied with the same number of hidden layers of the network, resulting in one hidden layer. The load step classification results of the ANN with the optimized structure are shown in figures 3.15 and 3.16. The target class refers to the actual label of the load step that causes the acoustic emission signal. The output class refers to the index of

the load step that is predicted by the ANN.
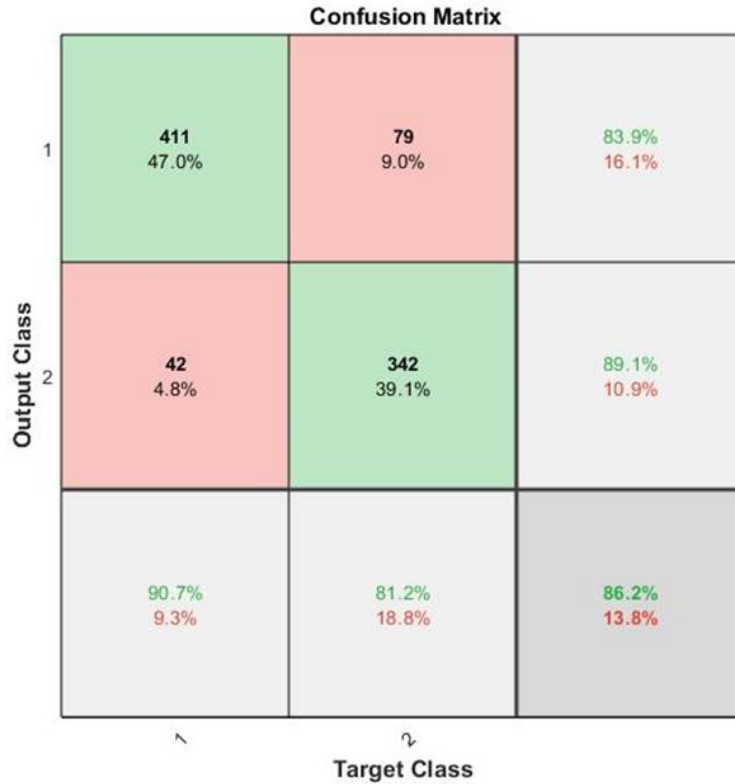
Confusion Matrix

Figure 3.15 Confusion Matrix for ANN

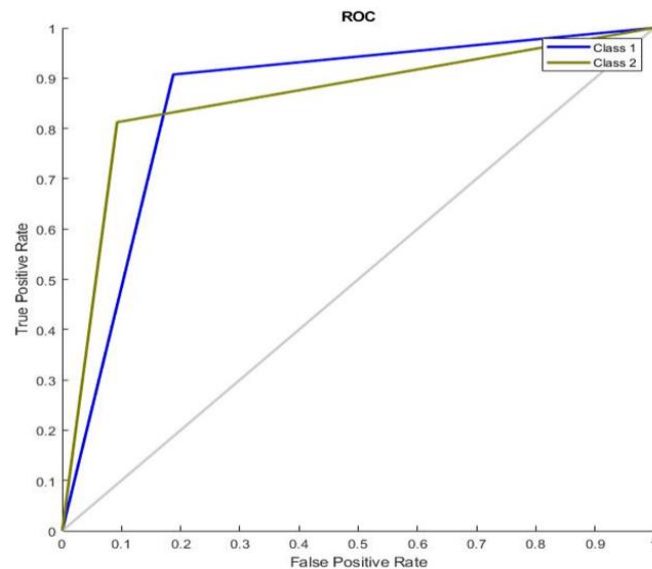**Figure 3.16 Receiver Operating Characteristic Curve for ANN**

The results from the ANN model show an overall accuracy of 86.2%, with 90.7% accuracy for the classification of load step 2 and 81.2% accuracy for the classification of load step 3. Class

Center for Connected Multimodal Mobility (C²M²)
Clemson University, Benedict College, The Citadel, South Carolina State University, University of South Carolina

19

1 refers to load step 2, while class 2 refers to load step 3. The neural network was helpful in classifying the random dataset taken from the training data.

This method demonstrates the ability to classify AE data into 10-kip load step categories. In the future, studies should be pursued to decrease the load steps from a 10 kip load step to a 2 kip load step. Because AE attributes change based on material properties, it is necessary to develop a large database of training data for the ANN to improve accuracy. This method may prove useful in damage detection as more data is collected.

3.5 Field investigation

A field investigation was conducted on January 20th, 2022, on a two-lane bridge (S-97) over Johnson Creek near Abbeville, SC (Figure 3.17). The span shown in Figure 3.18 was selected for monitoring, and the first interior panels (as shown in Figure 3.19) were instrumented with two strain gauges and four AE sensors. All devices were powered by solar panels (300 watts).

Figure 3.17 S-97 bridge near Abbeville, SC

Figure 3.18 Selected span for a monitoring
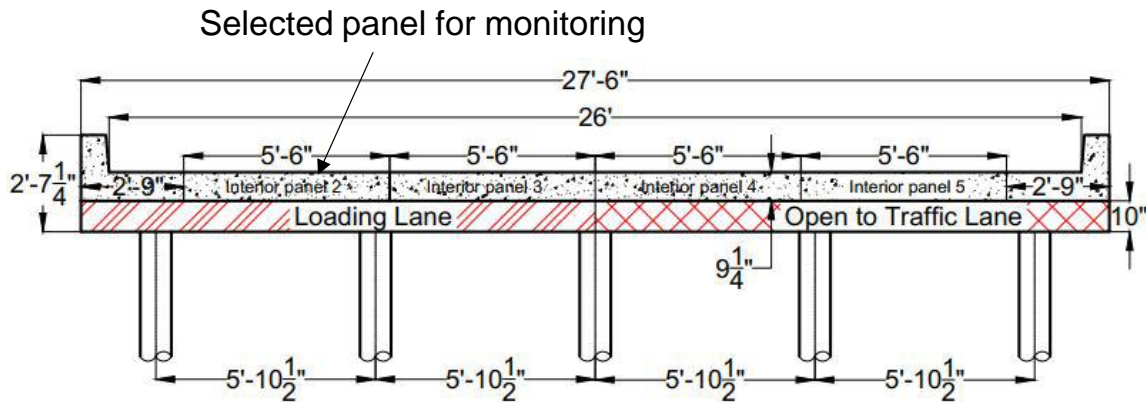
Figure 3.19 S-97 Cross section of the bridge and selected panel

Two strain gauges were adhered to the bottom of the panel, as shown in figure 3.20. Four AE sensors were adhered to the bottom of the panel at locations L/3 and W/3. The threshold was selected as 35 dB. Other settings were selected as follows: pre-trigger time = 256 μs; sampling rate = 1 MHz; peak definition time = 200 μs; hit definition time = 400 μs; hit lockout time = 200 μs.

Center for Connected Multimodal Mobility (C²M²)
Clemson University, Benedict College, The Citadel, South Carolina State University, University of South Carolina

21

Figure 3.20 AE sensors and strain gauges attached to the selected panel

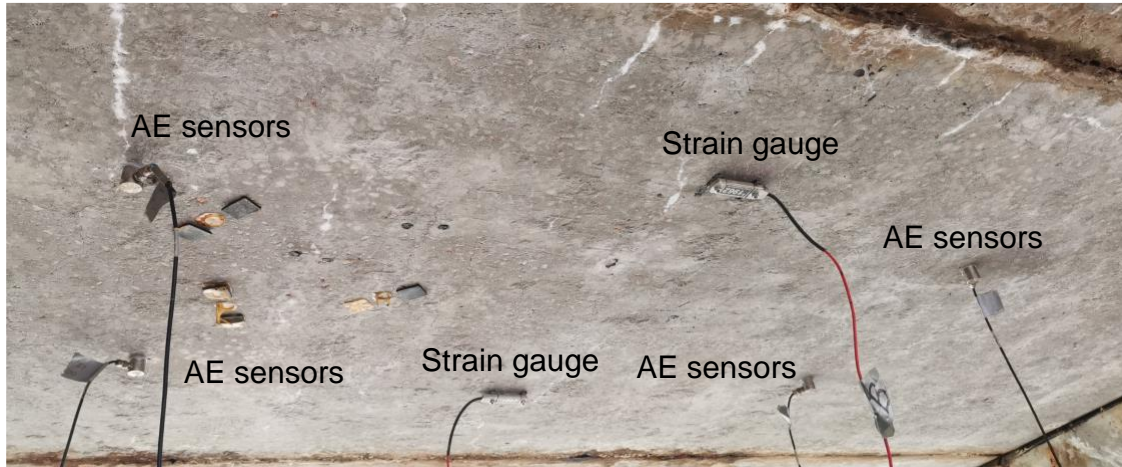Both strain and AE sensors recorded data while the vehicles were passing through the bridge. Figure 3.21 shows the relationship between the strain and AE data under loads for two consecutive vehicles. AE is a measure of damage such as crack formation and crack propagation; consequently, a linear relationship between acoustic emission data and strain measurements is not expected. AE sensors and strain gauges captured data from the first vehicle, while only the AE sensors can capture data from the second vehicle due to the inherent sensitivity of this sensor type.
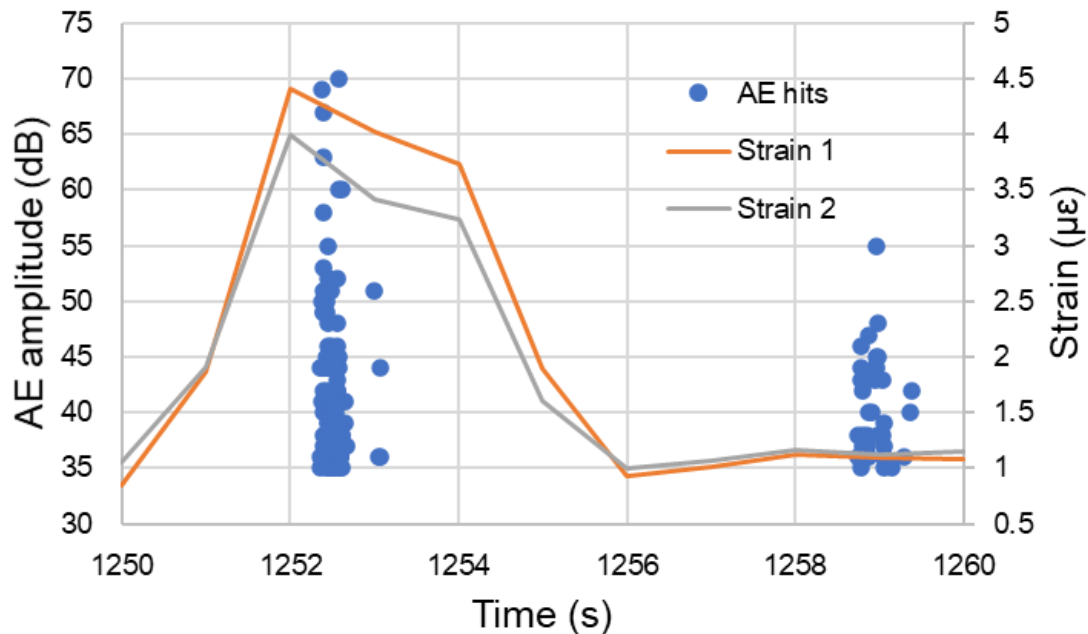

Figure 3.21 AE data activity and strain

Center for Connected Multimodal Mobility (C²M²)
Clemson University, Benedict College, The Citadel, South Carolina State University, University of South Carolina

22

In the case of monitoring of the bridge using AE sensors for an extended time period, the annual average daily traffic (ADTT) could be obtained, which may then be utilized to determine the live load factor γ_{DC} in the Load and Resistance Factor Rating (abbreviated as LRFR) equation as discussed further in Chapter 4. In addition, recorded AE signals may be employed to estimate loads of the passing vehicles by leveraging the machine learning model introduced in Section 3.4. The loads identified through AE, in combination with strain readings, may be used to update the FE model of the bridge span.

The AE signals and strains recorded during the field investigation were compared with the experimental results (Figure 3.22). The maximum strain captured by the strain gauges was 4.5 με (Figure 3.22a). This strain was recorded under a moving vehicle load (1998 Chevrolet Silverado, maximum 4,836 lbs) with a speed of 40 miles per hour. The maximum strain captured during the experiment was 101 με (Figure 3.22b), which was recorded under the load provided by the hydraulic ram (maximum 10,000 lbs). In this case, relatively more AE data was recorded in the actual bridge under a much reduced level of strain when compared to the laboratory investigation. This may potentially be due to the presence of shear between the joints; friction between the tires and the slab; and impact due to the moving load.

(a)

(b)
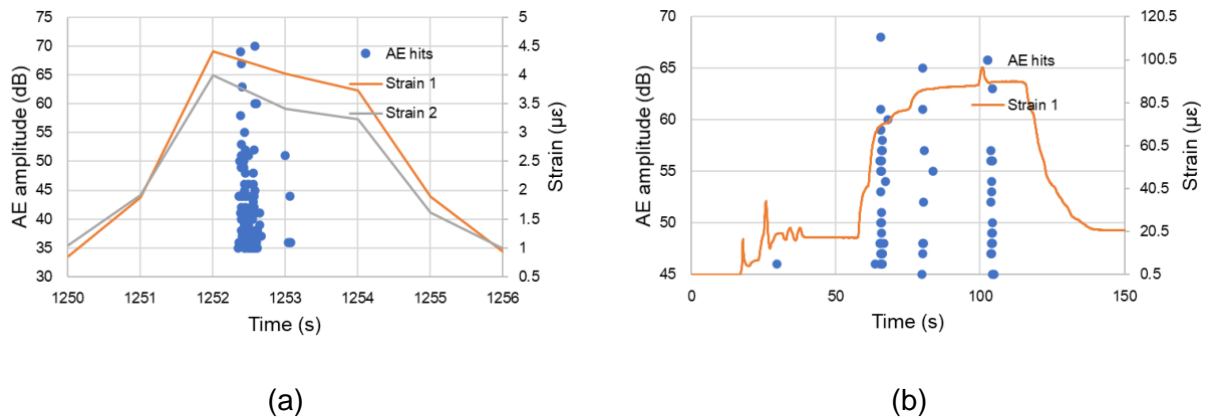
Figure 3.22 Comparison of results: (a) field investigation; (b) experiment

Center for Connected Multimodal Mobility (C²M²)
Clemson University, Benedict College, The Citadel, South Carolina State University, University of South Carolina

23

Chapter 4:
Result

A load rating procedure incorporating a modified digital twin approach is described in this chapter.

4.1 Load Rating Procedure Using Digital Twin

The procedure was developed for a two-lane bridge (S-97) over Johnson Creek near Abbeville, SC. The overall workflow is presented schematically in Figure 4.1. Strain transducers, potentiometers, and acoustic emission sensors were deployed on the bridge to capture the overall behavior of the bridge under traffic loading. A numerical model of the span was developed compared to readings of the strain gauges and potentiometers deployed on the bridge. While acoustic emission data is shown in the figure and is envisioned to be incorporated for future load ratings, this approach extends beyond the scope of the current study.
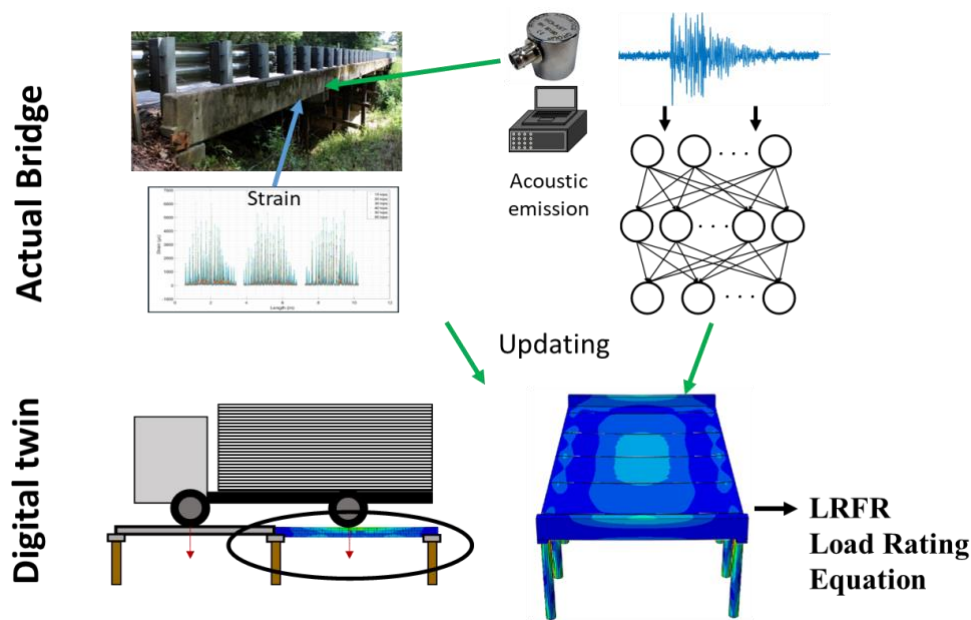

Figure 4.1 Workflow of the proposed load rating approach

For traditional load rating procedures in South Carolina, an LRFR equation (SCDOT 2019) was employed to investigate the rating factor for the flat slabs in the span. This equation is presented in Eq. (1):

$$RF = \frac{\phi_c \phi_s \phi R_n - \gamma_{DC} D_C - \gamma_{Dw} D_w}{\gamma_L L(1 + IM)} \tag{1}$$

Terminology is as follows: RF = load rating factor; ϕ_c = health condition; ϕ = resistance factor; R_n = nominal member resistance; ; γ_{DC} = permanent load factor; Dc = permanent load effect; γ_{DW} = dead weight factor (wearing surface); Dw = dead load effect (wearing surface and

utilities); L = live load effect (vehicle); IM = dynamic amplification; and γ_L = live load factor. The wearing surface and utilities were not considered, therefore γ_{DW} and Dw are not used.

For the proposed load rating procedure using a digital twin, a modified LRFR equation is proposed for investigation to calculate the load rating factor. The equation is presented in Eq. (2):

$$RF = \frac{\phi_c \phi_s \phi R_{n-FE} - D_C - D_w}{\gamma_L L_{FE}(1 + IM)} \tag{2}$$

where R_{n-FE} is the ultimate moment capacity derived by the FE model and L_{FE} is the live load effect calculated by the FE model.

In a traditional load rating approach, R_n is obtained by calculation, and the live load effect, L, is calculated considering the vehicle load and distribution factor. In the proposed load rating procedure, R_{n-FE} is obtained by an FE single slab model which is calibrated to the experimental test. The live load effect L_{FE} is calculated by the FE bridge span model. The purpose of the modified LRFR equation is to minimize factors that reflect uncertainties, such as the permanent load factor γ_{DC}, as the dead load is understood based on the dimensions and density of the reinforced concrete.

4.2 Results

This section presents a preliminary case study of the proposed load rating approach that is augmented through load testing of a specific bridge span. The bridge span described earlier was utilized to carry out the proposed load rating procedure. An FE span model (Figure 4.2) was developed and calibrated through readings obtained from strain gauges and potentiometers from a previously published report (Ziehl et al., 2020) and from measurements taken during a field visit in 2022.
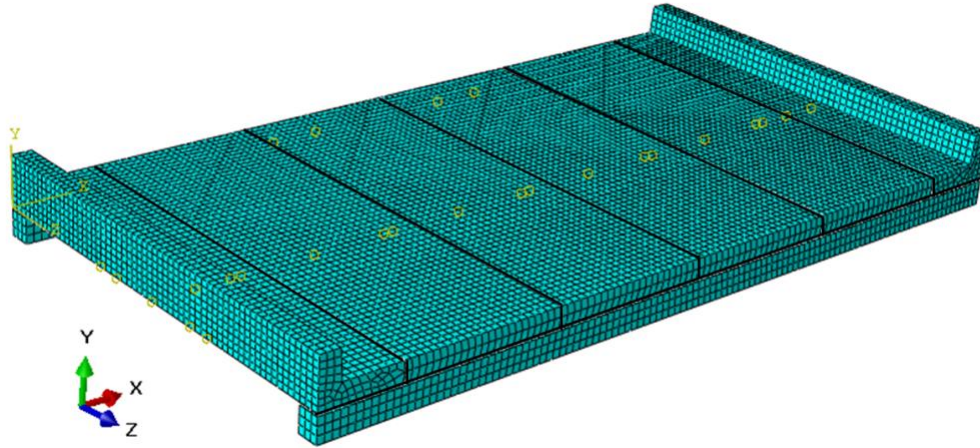

Figure 4.2 Detail of the modeled span

The single slab model introduced above was calibrated through an experimental test carried out in the laboratory. The slab was 15 feet in length, 5.5 feet in width, and 8.25 inches in depth.

However, the depth of the slab in the actual bridge is 9.25 inches. Therefore, the single slab model was updated to account for actual dimensions, and the span model was then assembled.

The span model was calibrated through a field investigation (Ziehl et al., 2020) through the loading of a heavy truck (supplied by SCDOT) of known dimensions and axle weights. The specific truck weight and dimensions are shown in Figure 4.3.
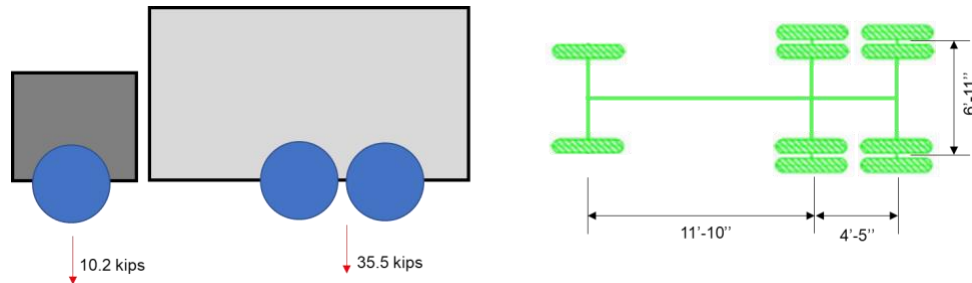

Figure 4.3 Truckload

During loading, strain gauges were attached, as shown in Figure 4.4. Strain readings with the truck in positions 1 through 3 were compared with strains obtained from the FE span model. Truck positions 1 through 3 are presented in Figure 4.5.
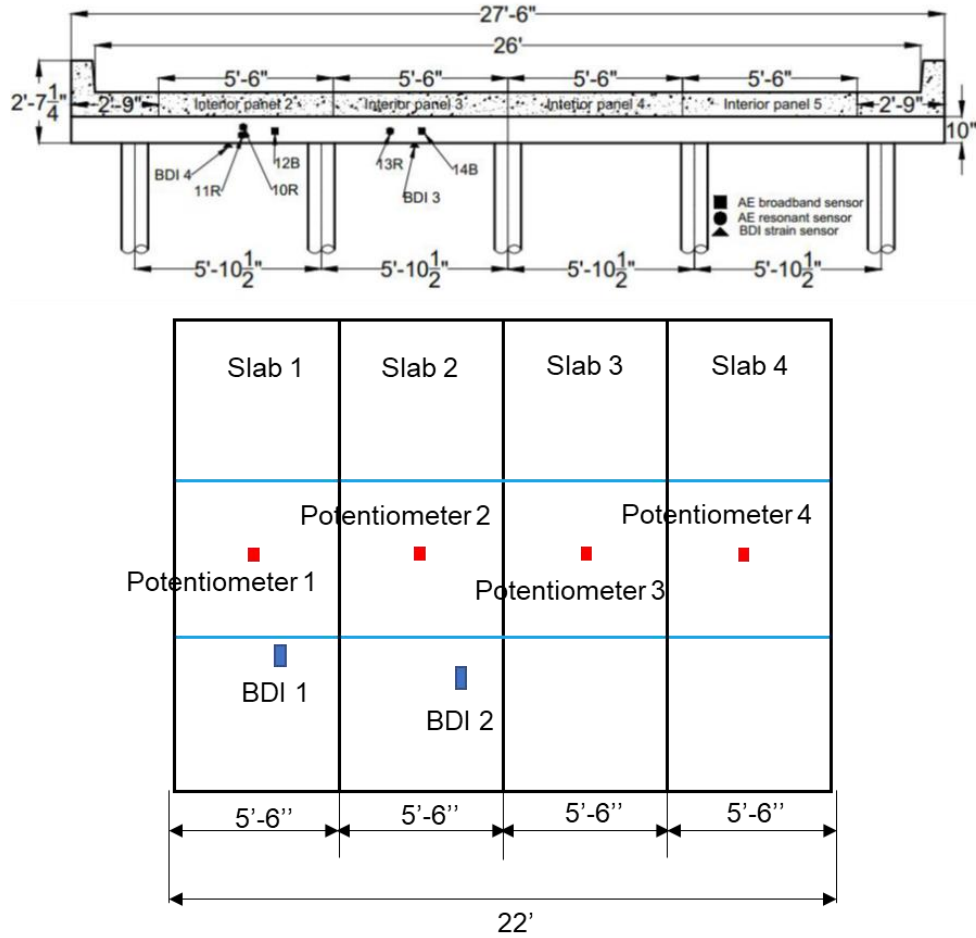
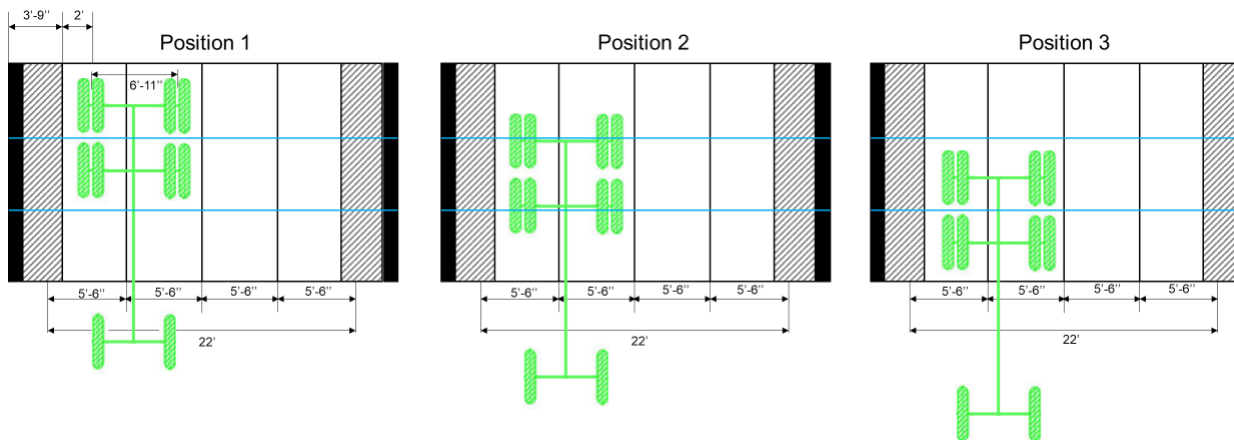**Figure 4.4 Detail of the span and BDI strain gauges layout**

Figure 4.5 Truck positions

Although differences were noted, the strains obtained by the FE bridge span model at the three truck positions were similar to those on the actual bridge span. In addition to strain, the maximum deflection of each slab in the FE span model was also compared, with the maximum deflection of each slab approximately corresponding to the deflection of the actual bridge. Thus, indicating that the load distribution between slabs in the FE model is similar to that of the actual bridge span.
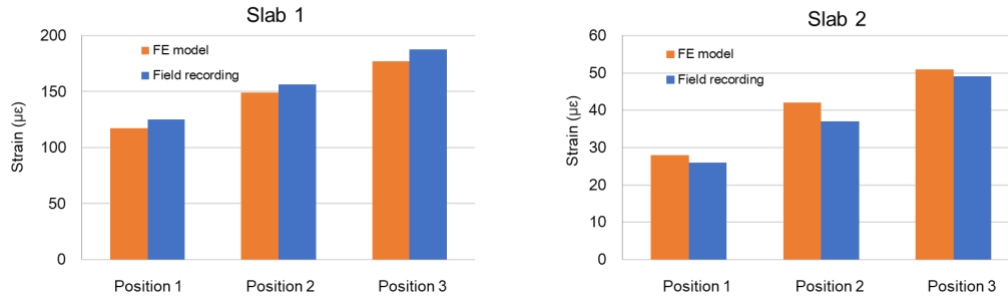
Figure 4.6 Strain calibration for slab 1 and slab 2
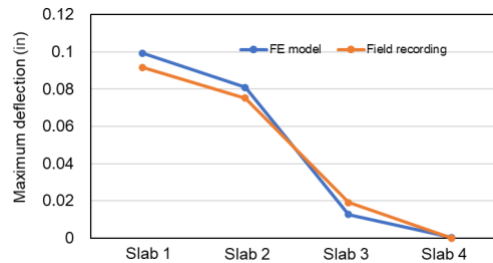
Figure 4.7 Calibration of deflection

The calibrated FE span model was then utilized to conduct a load rating for an H20 truck (weight and dimensions are shown in Figure 4.8). The truck position shown in Figure 4.9 was adopted.

Figure 4.8 Truckload of H20

Center for Connected Multimodal Mobility (C²M²)
Clemson University, Benedict College, The Citadel, South Carolina State University, University of South Carolina

28

Figure 4.9 H20 truck positions

For the traditional load rating approach (Eq. 1), material properties of 4,000 f'c and 40,000 psi fy were utilized, as these are the properties noted on the bridge drawings. A concrete cover of 1.5 inches was also assumed, as was a concrete density of 150 pcf which includes the steel reinforcement. The amount of steel reinforcement in the longitudinal direction was assumed to be (13) No. 7 bars c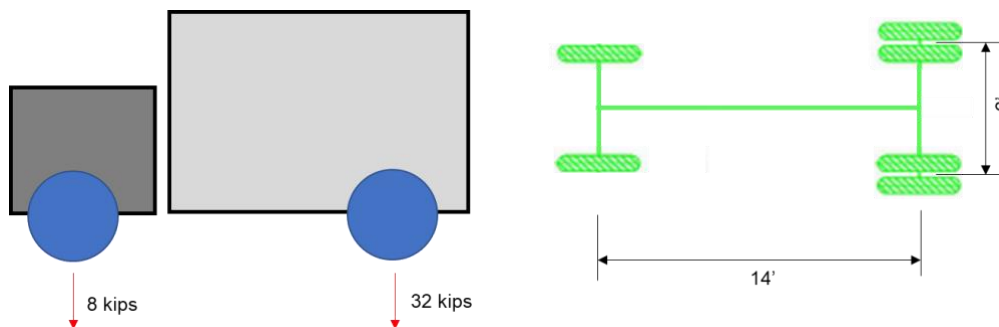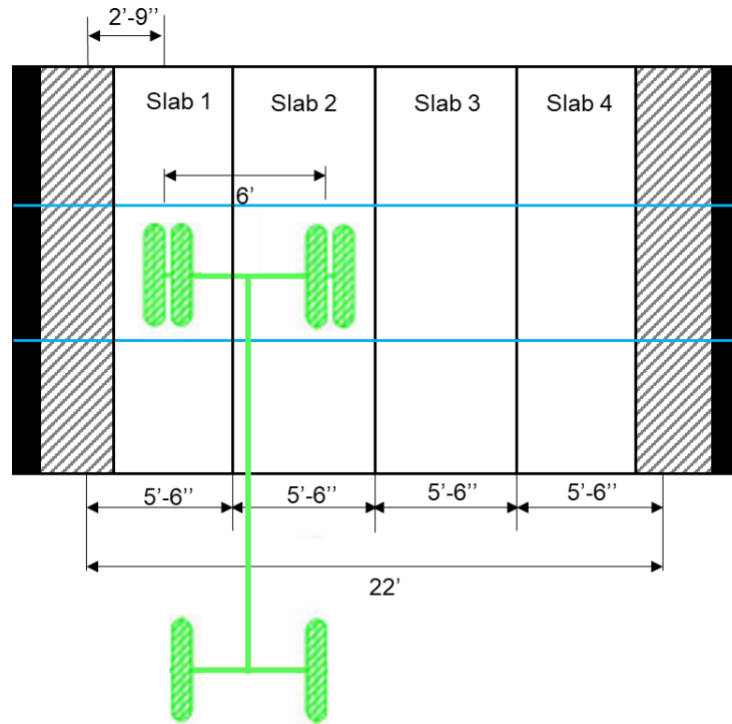onsistent with the plans. These assumptions resulted in an R_n value of 172 ft-kips. A distribution factor of 0.5 was also assumed in keeping with common assumptions for this bridge type in South Carolina. The dead load factor γ_{DC} was selected as 1.25 for the reinforced concrete bridge type. An inventory level evaluation was considered, and the live load factor γ_L was selected as 1.75 for limit state strength 1 (AASHTO, 2021).

To conduct a modified digital twin load rating approach, the laboratory investigation of the 8.25 in. thick slab was utilized. For this specimen, the measured moment capacity of 253 ft-kips was higher than expected when the traditional assumptions for material properties listed above were incorporated. While demolition and testing of the reinforcement for this slab were beyond the budgetary constraints, sampling from similar slabs indicated reinforcement yield stress in the range of 55,000 psi and f'c values in the range of 4,500 to 6,500 psi. The following values were utilized to match the measured moment capacity for the 8.25 in. thick slab tested in the laboratory: 5,000 psi f'c, 50,000 psi fy, cover = 1.0 in., longitudinal reinforcement = (13) No. 8 bars. These assumptions were also utilized for the 9.25 in. thick precast reinforced concrete slab in the Abbeville Bridge, resulting in an R_n value of 290 ft-kips. These assumptions, though potentially realistic, may be overly hopeful as the drawings call for No. 7 bars (as opposed to No. 8 bars),

Center for Connected Multimodal Mobility (C²M²)
Clemson University, Benedict College, The Citadel, South Carolina State University, University of South Carolina

29

therefore the calculation for R_n was also conducted for (13) No. 7 bars, leading to an R_n value of 231 ft-kips. These values are shown under the Digital Twin Load Rating column in Table 4.1.

The other factors affecting the load rating are the live load effect (L_{FE} value), where the effect of live load distribution found from the FE model is somewhat smaller than for the traditional approach, and the γ_{DC} factor, where the dead load effect is well understood in the digital twin approach. Therefore, this factor is not considered.

Table 4.1 Comparison of the load rating results

	Traditional Load Rating	Digital Twin Load Rating	
Slab	1	1	1
$\mathbf{R_n}$ **(ft − kips)**	172	231	290
$\mathbf{D_C}$ **(ft − kips)**	17.9	17.9	17.9
LL, L_{FE} (ft - kips)	60	53.7	54.1
IM	0.33	0.33	0.33
γ_{DC}	1.25	/	/
$\boldsymbol{\gamma_L}$	1.75	1.75	1.75
$\boldsymbol{\phi_C}$	0.85	0.85	0.85
$\boldsymbol{\phi}$	0.9	0.9	0.9
$\boldsymbol{\phi_s}$	1	1	1
Load Rating Factor	0.78	1.27	1.62

As mentioned above, the precast reinforced concrete flat slab specimen that was tested in the laboratory demonstrated higher strength than calculated when conventional assumptions for materials, such as f'c of 4,000 psi and fy of 60,000 psi, were incorporated. Future studies will include the testing of additional precast reinforced concrete flat slab specimens to better understand the increase in tested flexural capacity. It will also include the sampling of the materials in the specimens with a focus on the steel reinforcement as well as the concrete cover.

CHAPTER 5:
Conclusions and Discussion

A Digital Twin (DT) approach toward load rating has been described. This approach provides an alternative methodology for load rating of precast reinforced flat slab bridges. The DT model was developed based on an experimental laboratory study, numerical simulations, a load test with trucks of known axle weight and dimensions, and field investigations under normal traffic loading. The load rating factor was calculated through the LRFR load rating procedure and a modified digital twin load rating procedure.

Conclusions

Conclusions are summarized as follows:

- The digital twin approach to load rating resulted in an increased numerical value for load rating in the case studied. The increase in the rating factor is attributable to a) a higher ultimate moment capacity of the slab studied, b) a lower live load effect derived from the FE bridge span model, and c) a decrease in the dead load factor.

- Artificial Neural Networks (ANN) show promise for the classification of AE data for this application. AE data is different from strain and displacement data in the sense that a) it is more sensitive to the passage of minor loads, such as cars and SUVs, on the bridge, and b) it is inherently sensitive to damage growth due to a number of sources including corrosion of the steel reinforcement. The differences in the nature of AE data when compared to strain and displacement data suggest that it may be useful as a supplemental method to strain and displacement data. It may also be potentially used in a data fusion approach to develop a health index for a bridge span or spans.

- The limitation of using ANN for the classification of AE data is that the training data, regardless of diversity. For example, only data from two load steps were used for training, and in addition, ANN only used data from one slab. Future work should have ANN trained by more load steps and smaller step sizes. Future work should also involve data on different slabs into the training and validation of ANN to further investigate the generalization performance of this method.

Discussion

Minor differences were noticed between the field measurements under moving load and those predicted by the FE model of the bridge span. Future work should conduct more field experiments to investigate the statistical significance of this difference. Once the statistical significance of the differences can be verified, future work should also include the effects of moving loads in the FE modeling, including the effect of impact. The DT procedure would benefit from additional data gathered both during testing and in the field.

The precast reinforced concrete flat slab specimen that was tested in the laboratory demonstrated higher strength than calculated when conventional assumptions for materials, such as f'c of 4,000 psi and fy of 60,000 psi, were incorporated. One potential explanation for this is that No. 8 reinforcing bars may have been used in place of No. 7 reinforcing bars. This type of anomaly is common and is one of the challenges associated with understanding this bridge type. While beyond the scope of this investigation, future studies will include the testing of additional

precast reinforced concrete flat slab specimens to better understand the increase in tested flexural capacity and sampling of the materials in the specimens. A longer-term monitoring period in the field will also be pursued so that vehicular loading of the bridge may be better understood, including the effects of moving loads on the impact factor and the average daily truck traffic. Future studies will also incorporate variability associated with materials properties that may be found throughout the state.

References

AASHTO (2019). Manual for bridge evaluation, 2nd Ed., Washington, D.C., 2019.

AASHTO (2021). Manual for bridge evaluation, 3rd Ed., Washington, D.C., 2021.

Aguilar, C. V., Jáuregui, D. V., Newtson, C. M., Weldon, B. D., & Cortez, T. M. (2015). Load rating a prestressed concrete double T-beam bridge without plans by field testing. Transportation Research Record, 2522(1), 90-99.

Alampalli, S., Frangopol, D. M., Grimson, J., Halling, M. W., Kosnik, D. E., Lantsoght, E. O., ... & Zhou, Y. E. (2021). Bridge load testing: State-of-the-practice. Journal of Bridge Engineering, 26(3), 03120002.

Anay, R., Cortez, T. M., Jáuregui, D. V., ElBatanouny, M. K., & Ziehl, P. (2016). On-site acoustic-emission monitoring for assessment of a prestressed concrete double-tee-beam bridge without plans. Journal of Performance of Constructed Facilities, 30(4), 04015062.

ARTBA (2020), Bridge Report. American Road & Transportation Builders Association (ARTBA).

ASCE (2013). Report card on America's infrastructure, Reston, VA.

ASCE (2017) Infrastructure Report Card, https://infrastructurereportcard.org/new-bridge-data-supports-c-report-card-grade/

Butler, L. J., Lin, W., Xu, J., Gibbons, N., Elshafie, M. Z., & Middleton, C. R. (2018). Monitoring, modeling, and assessment of a self-sensing railway bridge during construction. Journal of Bridge Engineering, 23(10), 04018076.

Casas, J. R., & Gómez, J. D. (2013). Load rating of highway bridges by proof-loading. KSCE Journal of Civil Engineering, 17(3), 556-567.

Din-Houn Lau, F., Butler, L. J., Adams, N. M., Elshafie, M. Z., & Girolami, M. A. (2018). Real-time statistical modelling of data generated from self-sensing bridges. Proceedings of the Institution of Civil Engineers-Smart Infrastructure and Construction, 171(1), 3-13.

Fu, G., Pezze III, F. P., & Alampalli, S. (1997). Diagnostic load testing for bridge load rating. Transportation research record, 1594(1), 125-133.

Hernandez, E. S., & Myers, J. J. (2018). Diagnostic test for load rating of a prestressed SCC bridge. Special Publication, 323, 11-1.

Islam, A. A., Jaroo, A. S., & Li, F. (2015). Bridge load rating using dynamic response. Journal of Performance of Constructed Facilities, 29(4), 04014120.

Kim, Y. J., Tanovic, R., & Wight, R. G. (2009). Recent advances in performance evaluation and flexural response of existing bridges. Journal of performance of constructed facilities, 23(3), 190-200.

Lantsoght, E. O., van der Veen, C., de Boer, A., & Hordijk, D. A. (2017b). State-of-the-art on load testing of concrete bridges. Engineering Structures, 150, 231-241.

Lantsoght, E., van der Veen, C., de Boer, A., & Hordijk, D. A. (2017a). Proof load testing of reinforced concrete slab bridges in the Netherlands. Structural Concrete, 18(4), 597-606.

Lin, W., Butler, L. J., Elshafie, M. Z., & Middleton, C. R. (2019). Performance assessment of a

newly constructed skewed half-through railway bridge using integrated sensing. Journal of Bridge Engineering, 24(1), 04018107.

Liu, Z., Bai, W., Du, X., Zhang, A., Xing, Z., & Jiang, A. (2020). Digital twin-based safety evaluation of prestressed steel structure. Advances in Civil Engineering, 2020.

Lu, Q., Parlikad, A. K., Woodall, P., Don Ranasinghe, G., Xie, X., Liang, Z., ... & Schooling, J. (2020). Developing a digital twin at building and city levels: Case study of West Cambridge campus. Journal of Management in Engineering, 36(3), 05020004.

MISTRAS Group, https://www.mistrasgroup.com/company/branches/princeton-junction-nj-usa/

SCDOT (2019), Load Rating Guidance Document

Shim, C. S., Dang, N. S., Lon, S., & Jeon, C. H. (2019a). Development of a bridge maintenance system for prestressed concrete bridges using 3D digital twin model. Structure and Infrastructure Engineering, 15(10), 1319-1332.

Shim, C. S., Kang, H. R., & Dang, N. S. (2019). Digital twin models for maintenance of cable-supported bridges. In International Conference on Smart Infrastructure and Construction 2019 (ICSIC) Driving data-informed decision-making (pp. 737-742). ICE Publishing.

Ye, C., Butler, L., Bartek, C., Iangurazov, M., Lu, Q., Gregory, A., ... & Middleton, C. (2019, September). A digital twin of bridges for structural health monitoring. In 12th International Workshop on Structural Health Monitoring 2019. Stanford University.

Ziehl, P., Cousins, T., Ross, B., & Huynh, N. (2020). Assessment of structural degradation for bridges and culverts (No. FHWA-SC-20-03). South Carolina. Dept. of Transportation. Office of Materials and Research.

Zulifqar, A., Cabieses, M., Mikhail, A., & Khan, N. (2014). Design of a bridge inspection system (BIS) to reduce time and cost. George Mason University: Farifax, VA, USA.